Phase Transformations in Mesostructured Silica/Surfactant Composites. Mechanisms for Change and Applications to Materials Synthesis†

Christopher C. Landry,*,‡ Sarah H. Tolbert,§ Karl W. Gallis,‡ Alain Monnier,†,|| Galen D. Stucky,⊥ Poul Norby,#,○ and Jonathan C. Hanson○

Department of Chemistry, University of Vermont, Burlington, Vermont, 05405, Department of Chemistry and Biochemistry, University of California, Los Angeles, California 90095, Departement de Chimie Physique Sciences II, l'Université de Genève, 1211 Geneva, Switzerland, Departments of Chemistry and Materials, University of California, Santa Barbara, California 93106, Department of Chemistry, University of Oslo, N-0315 Oslo, Norway, Department of Chemistry, Brookhaven National Laboratory, Upton, New York 11973

Received May 5, 2000. Revised Manuscript Received January 13, 2001

In this study, phase transformation of the hexagonal mesostructure MCM-41 to the cubic mesostructure MCM-48 is examined by in situ X-ray diffraction (XRD) of the transforming mesostructure and by XRD of products from bulk transformation experiments in Parr autoclaves. Transformations were studied under conditions of high pH and temperatures between 100 and 190 °C. Heating events took place after the hexagonal mesophase had assembled, but before it had fully polymerized. On the basis of these and previous results on transformations in silica−surfactant−water and surfactant−water systems, a model is proposed to explain the expected hexagonal → cubic transformation as well as the brief existence of a lamellar phase during the transformation. Additional experiments to establish synthetic parameters for the transformation included varying the silicon alkoxide source, replacing the supernatant prior to heating, and adding fluoride or aluminum to the reaction mixture. The results, taken together, illustrate the strong cooperativity between the organic and inorganic regions in controlling the assembly of the mesostructure and provide a better understanding of the effects that control phase transformations in these systems.

Introduction

Ordered forms of mesoporous materials may be synthesized in a variety of hexagonal, cubic, and lamellar phases.[1−4] Silicate and aluminosilicate forms of these materials are made by a self-assembly process in either acidic or basic solution, which is driven by charge-matching considerations between a surfactant assembly and the polymerizing inorganic framework.[3,5] The crystallographic phases found for these materials often (but not always)[6] mimic the phases found for the surfactants in water. Much attention has been focused on the hexagonal (MCM-41, plane group *p*6*m*) phase, which is synthesized in basic solution, most likely due to the relative difficulty in preparing the other phases. However, many other mesoporous phases have more potential for use in such applications as catalysis, ion exchange, and chromatography.[7] For example, MCM-48, which has a highly branched and interwoven bicontinuous pore structure (space group *Ia*3*d*) is an attractive candidate for the above applications since reactant

* To whom correspondence should be addressed. E-mail: cclandry@zoo.uvm.edu. Internet: http://www.uvm.edu/~chemdept/landry.html.

† This paper is dedicated to the memory of our colleague and friend Alain Monnier, whose passing has left a gap in the scientific community. His insight and expertise has had a profound effect on this work and he is sorely missed.

‡ University of Vermont.
§ University of California, Los Angeles.
|| L'Université de Genève.
⊥ University of California, Santa Barbara.
University of Oslo.
○ Brookhaven National Laboratory.

(1) (a) Kresge, C. T.; Leonowicz, M. E.; Roth, W. J.; Vartuli, J. C.; Beck, J. S. *Nature* **1992**, *359*, 710. (b) Beck, J. S.; Vartuli, J. C.; Roth, W. J.; Leonowicz, M. E.; Kresge, C. T.; Schmitt, K. D.; Chu, C. T.−W.; Olson, D. H.; Sheppard, E. W.; McCullen, S. B.; Higgins, J. B.; Schlenker, J. L. *J. Am. Chem. Soc.* **1992**, *114*, 10834. (c) Zhao, D.; Feng, J.; Huo, Q.; Melosh, N.; Frederickson, G. H.; Chmelka, B. F.; Stucky, G. D. *Science* **1998**, *279*, 548.

(2) Huo, Q.; Leon, R.; Petroff, P. M.; Stucky, G. D. *Science* **1995**, *268*, 1324.

(3) Huo, Q.; Margolese, D. I.; Stucky, G. D. *Chem. Mater.* **1996**, *8*, 1147.

(4) Monnier, A.; Schüth, F.; Huo, Q.; Kumar, D.; Margolese, D.; Maxwell, R. S.; Stucky, G. D.; Krishnamurty, M.; Petroff, P.; Firouzi, A.; Janicke, M.; Chmelka, B. F. *Science* **1993**, *261*, 1299.

(5) (a) Huo, Q.; Margolese, D. I.; Ciesla, U.; Demuth, D. G.; Feng, P.; Gier, T. E.; Sieger, P.; Firouzi, A.; Chmelka, B. F.; Schüth, F.; Stucky, G. D. *Chem. Mater.* **1994**, *6*, 1176. (b) Firouzi, A.; Kumar, D.; Bull, L. M.; Besier, T.; Sieger, P.; Huo, Q.; Walker, S. A.; Zasadzinski, J. A.; Glinka, C.; Nicol, J.; Margolese, D.; Stucky, G. D.; Chmelka, B. F. *Science* **1995**, *267*, 1138. (c) Stucky, G. D.; Monnier, A.; Schüth, F.; Huo, Q.; Margolese, D. I.; Kumar, D.; Krishnamurty, M.; Petroff, P.; Firouzi, A.; Janicke, M.; Chmelka, B. F. *Mol. Cryst. Liq. Cryst.* **1994**, *240*, 187. (d) Huo, Q.; Margolese, D. I.; Ciesla, U.; Feng, P.; Gier, T. E.; Sieger, P.; Leon, R.; Petroff, P. M.; Schüth, F.; Stucky, G. D. *Nature* **1994**, *368*, 317.

(6) Lu, Y. F.; Ganguli, R.; Drewien, C. A.; Anderson, M. T.; Brinker, C. J.; Gong, W.; Guo, Y.; Soyez, H.; Dunn, B.; Huang, M. H.; Zink, J. I. *Nature* **1997**, *389*, 364.

(7) Gallis, K. W.; Araujo, J. T.; Duff, K. J.; Moore, J. G.; Landry, C. C. *Adv. Mater.* **1999**, *11*, 1452.

10.1021/cm000373z CCC: $20.00
Published on Web 04/13/2001

molecules could avoid pore blockages. This is in contrast to MCM-41, which consists of nonbranched pores.

Recently, a method was described by which MCM-48 could be synthesized through a phase transformation process.[8] The MCM-41/-48 transformation was performed by stirring a reaction mixture at room temperature for a short period of time to synthesize an incompletely polymerized mesostructure, followed by a heating step at an advanced temperature to induce structural change. Ethanol, formed by the hydrolysis of the silicate source TEOS (tetraethyl orthosilicate), was shown to drive the transformation by altering surfactant packing within the micellar surfactant templates. Other groups have also noted the effects of alcohols on pore structure, particle size, and particle shape in assembling silicate systems.[2,9]

The conclusions in previous studies were reached by simply taking powder X-ray diffraction (XRD) patterns before and after treatment. However, the structural relationships occurring during the transformation cannot be observed by this method. For example, epitaxial relationships between the corresponding liquid-crystalline phases, traditionally designated H_α and Q_α for the *p*6*m* and *Ia*3*d* phases, have been previously established.[10−13] Models producing expected unit cell parameters and micellar surface area/volume ratios at the phase transformation boundary have been proposed.[10] The similarities between the MCM-41/-48 and H_α/Q_α transformations implies that even after 2 h of polymerization, the inorganic region of the mesostructure is still sufficiently unpolymerized that surfactant packing considerations controlling rearrangements in the *organic* region of the mesostructure can be used to manipulate the ultimate pore geometries of mesoporous materials. The use of in situ XRD to study the development of mesostructures can provide important insight into their formation, which has been shown previously.[14] In situ XRD experiments allow analysis of the phase transformation as it is happening and thus can be used to determine conclusively whether the transformations occurring in the liquid-crystal systems mimic those in these composite systems. Moreover, since it is possible to form silicate mesostructures with phases that have no analogue in the liquid-crystal literature (for the surfactant being used), it may be possible to observe short-lived, metastable phases during the transformation process using in situ XRD. Finally, in situ diffraction can be used to extract thermodynamic and kinetic information regarding phase transformations, such as activation energy barriers. These data can be used to design synthetic conditions that will consistently produce the desired cubic phase.

In this report, we use in situ XRD to study the phase transformation of MCM-41 to MCM-48 under high pH conditions when the system responds to changes in surfactant packing. We also expand upon previous results[8] by illustrating that this process may be carried out at any temperature between 100 and 190 °C, as long as the polymerization time and heating times are adjusted appropriately. Finally, we provide additional data regarding the effects of alcohol partitioning on the phase transformation by using several silicon alkoxides other than TEOS as the silicate source and examine how the phase transformation proceeds when other inorganics such as aluminum and fluoride are added to the reaction system.

Experimental Section

Materials and Methods. Powder X-ray diffraction (XRD) experiments were performed on a Scintag X1 $\theta-\theta$ diffractometer equipped with a Peltier (solid-state thermoelectrically cooled) detector using Cu Kα radiation. Nitrogen adsorption and desorption isotherms were obtained on a Micromeritics ASAP 2010 instrument. Samples were degassed at 200 °C under vacuum overnight prior to measurement. Surface areas were measured using the BET (Brunauer−Emmett−Teller) method and pore size distributions were calculated from the BJH (Barrett−Joyner−Halenda) method. ^{27}Al and ^{29}Si MAS NMR spectra were obtained on a Bruker AM500. Samples were spun at 3.5 kHz. All chemicals were purchased from Aldrich and were used as received.

Silicate−Surfactant Reaction Mixtures. Typical conditions for performing the phase transformation have been previously described.[8] As was also reported previously, we have found that the phase transformation process is sensitive to experimental conditions; hence, attention must be paid to the order of addition of reactants, the size of the beaker relative to the stir bar, and the rate of stirring. We have obtained our most consistent results by adding NaOH as a 2 M solution to an amount of water, then adding surfactant and dissolving it by either heating or sonicating, allowing the solution to cool, and then adding the silicon alkoxide source. The final reactant ratio was SiO_2:NaOH:CTAB:H_2O = 8.41:4.21:1.00:991, regardless of the alkoxide source used. Additional reactants such as aluminum isopropoxide, NaF, NH_4F, and $NH_4F{\cdot}HF$ were added as described in the text, prior to addition of TEOS.

Bulk-Phase Transformations. After the silicate mixture was stirred for a fixed amount of time, the entire reaction mixture was transferred to a Teflon-lined steel Parr autoclave and heated to a temperature between 100 and 190 °C for another fixed time period. Exact conditions are given in the paper. After the autoclaves were cooled to room temperature, the white solid was collected by filtration, washed with distilled H_2O, and then air-dried prior to analysis.

Observation of Phase Transformation by In Situ XRD. In situ XRD phase transformations were performed at beamline X7B of the National Synchrotron Light Source at Brookhaven National Laboratory. Equipment used in performing in situ phase transformation experiments has been used in previously published experiments.[15] Reaction mixtures were made in beakers and then transferred to a small glass capillary that was open at one end. The capillary was mounted on a goniometer head and back pressure applied to the open end of the capillary tube, recreating hydrothermal conditions. Aqueous reaction mixtures can be examined at temperatures as high as 260 °C by adjusting the applied pressure. Hot air, at a temperature controlled by a thermocouple feedback system, was blown over the sample and diffraction began. Time

(8) Gallis, K. W.; Landry, C. C. *Chem. Mater.* **1997**, *9*, 2035.
(9) (a) Anderson, M. T.; Martin, J. E.; Odinek, J. G.; Newcomer, P. P. *Chem. Mater.* **1998**, *10*, 311. (b) Anderson, M. T.; Martin, J. E.; Odinek, J. G.; Newcomer, P. P. *Chem. Mater.* **1998**, *10*, 1490. (c) Grün, M.; Unger, K. K. *Proceedings of the 12th International Zeolite Conference*; Treacy, M. M. J., Marcus, B. K., Bisher, M. E., Higgins, J. B., Eds.; MRS Publishing: Warrendale, PA, 1999; Vol. 2, p 757. (d) Kim, J. M.; Kim, S. K.; Ryoo, R. *Chem. Commun.* **1998**, 259.
(10) Luzzati, V. *J. Phys. II France* **1995**, *5*, 1649.
(11) Mariani, P.; Amaral, L. Q.; Saturni, L.; Delacroix, H. *J. Phys. II France* **1994**, *4*, 1393.
(12) Clerc, M.; Levelut, A. M.; Sadoc, J. F. *J. Phys. II France* **1991**, *1*, 1263.
(13) Rançon, Y.; Charvolin, J. *J. Phys. Chem.* **1988**, *92*, 2646.
(14) McGehee, M. D.; Gruner, S. M.; Yao, N.; Chun, C. M.; Navrotsky, A.; Aksay, I. A. *Proc. 52nd Ann. Mtg. Microsc. Soc. Am.* **1994**, 448.
(15) Norby, P. *J. Am. Chem. Soc.* **1997**, *119*, 5215.

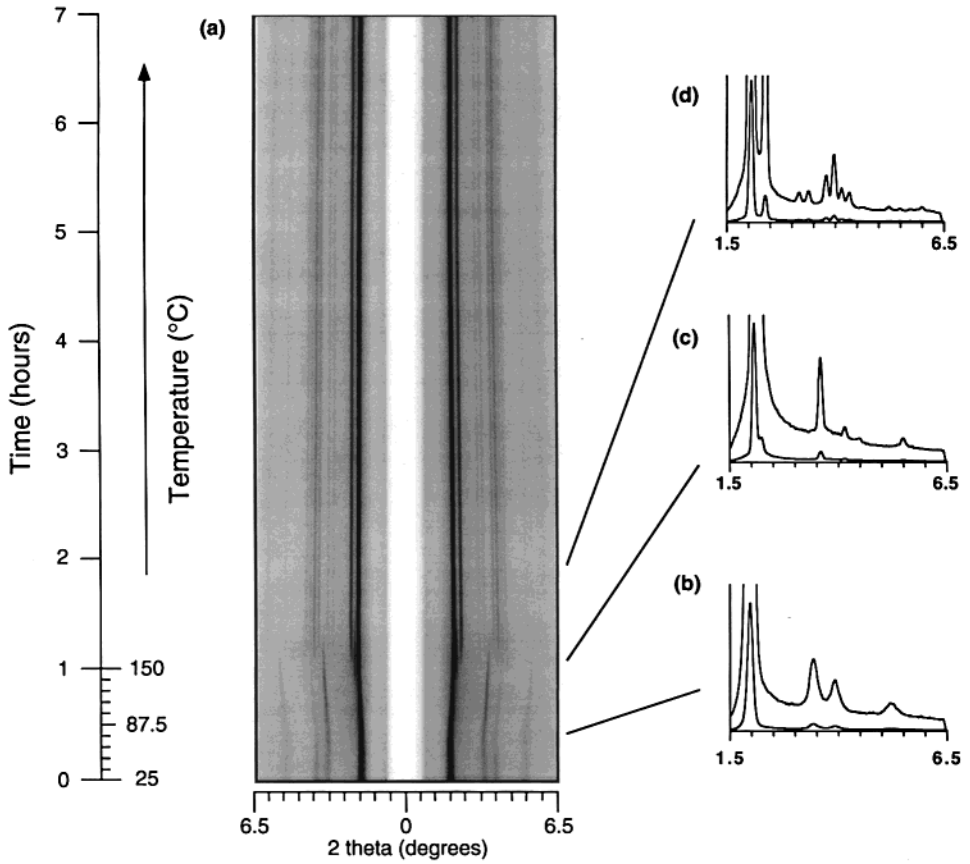

Figure 1. In situ X-ray diffraction patterns acquired as a function of time and temperature for a transforming mesostructure (high temperature = 150 °C). (a) Image plate showing time-resolved changes in scattering intensity (dark regions) that reflect mesophase morphologies and transformations directly; (b) hexagonal mesostructure present at low temperature (20.6 min, 68.0 °C); (c) mixture of hexagonal mesostructure and layered phases present as the phase transformation begins (60.0 min., 150 °C); (d) cubic mesostructure present at high temperature and after the phase transformation is complete (105.0 min, 150 °C). The thick white line in the center of the image plate is due to the beam stop. Scattering angle (2θ) vs intensity plots were obtained by taking the center of the beam stop as 0° and reading the intensity at each pixel on the right-hand side of the plate for a given *y* position. Lines are drawn to indicate the approximate position of each plot; indexing of the peaks in each phase is given in Table 1.

resolution was accomplished by moving the image plate at a fixed rate behind a metal slit; since heating could be carried out at a fixed rate, the process also accomplished temperature resolution. Diffraction from the sample appeared as streaks on the image plate, with phase changes appearing as new streaks arose and existing ones vanished.

Results and Discussion

In Situ XRD Experiments. An experiment was performed in which a reaction mixture was allowed to polymerize at room temperature for 3 h, then transferred to a capillary, ramped slowly to 150 °C over the course of an hour, and held at that temperature for an additional 7 h. Diffraction was taken during the heating process. Results from this experiment are shown in Figure 1. At room temperature, the as-synthesized sample shows a four-peak diffraction pattern consistent with the hexagonal *p*6*m* structure of MCM-41. The lattice parameter calculated from this pattern reflects structural periodicity with a characteristic length of approximately 47 Å, as expected for hexagonal arrays of cylindrical silicate−surfactant aggregates formed using cetyltrimethylammonium (CTA^+) species. Upon heating, however, the peaks sharpen and increase in intensity during the first 25 min. They then gradually show a decrease in *d*-spacing for another 35 min until soon after reaching 150 °C the (11) peak of MCM-41 disappears and many new peaks appear simultaneously. Some of the peaks that appear in the phase transformation region can be indexed to a lamellar phase while most of the peaks correspond to MCM-48. The phase changes occur more slowly and gradually than zeolitic transformations[15] or phase transformation of MCM-41 to a lamellar phase in neutral solution,[16] both studied by in situ XRD. The *d*-spacing of MCM-48 increases slightly over the remaining time of the experiment, but no further phase changes are recorded other than the disappearance of the lamellar phase.

What one notices immediately is the structural relationship between the MCM-41 and MCM-48 phases. The (10) and (20) reflections of MCM-41 transform smoothly into the (211) and (422) reflections of MCM-48. Previous X-ray and neutron scattering experiments on the analogous liquid-crystal systems (surfactant/water only) have shown a geometric correlation between the [10] planes of the H_α phase and the [211] planes of the Q_α phase.[10] In these previous discussions, this correlation was illustrated by observing the two phases aligned side by side, with the cylinder axis of the hexagonal phase

(16) Tolbert, S. H.; Landry, C. C.; Stucky, G. D.; Chmelka, B. F.; Norby, P.; Hanson, J. *Chem. Mater.*, submitted.

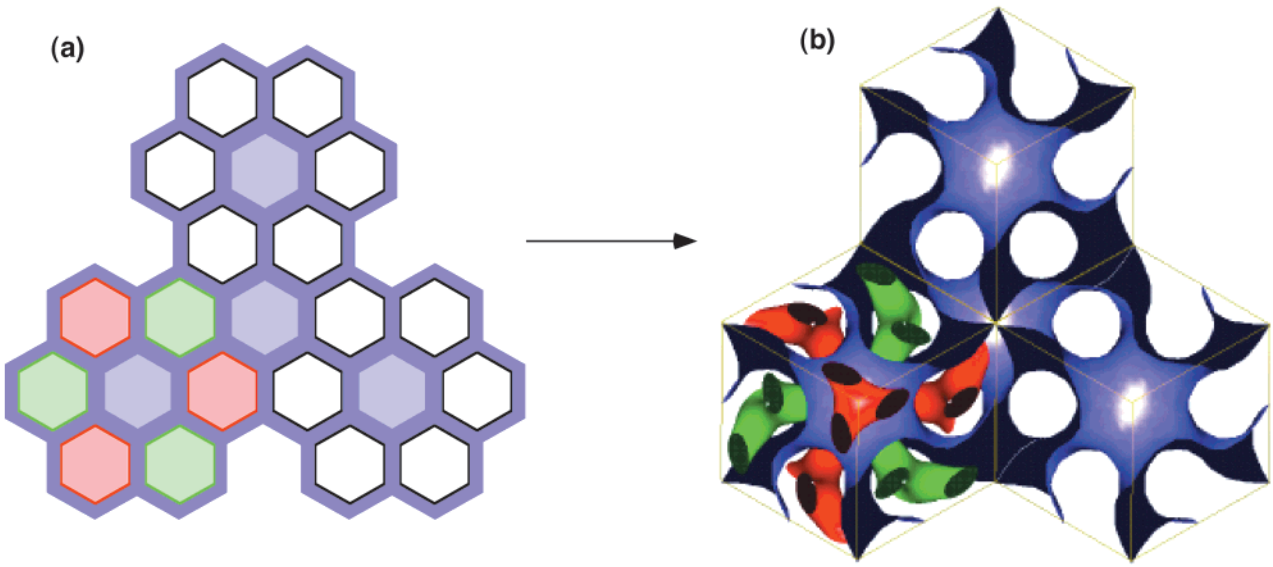

Figure 2. Possible correlation of pore structures in MCM-41 and MCM-48. (a) Several cylindrical pores of MCM-41 viewed along their axes; (b) four unit cells of MCM-48 viewed along the body diagonal [(111) direction] of the unit cell. Red and green coloring is used to indicate the correlation between pore structure of the hexagonal and cubic phases. The purple surface indicates the location of the silicate framework on the IPMS in the cubic mesostructure.

Table 1. Peak Indices and Unit Cell Parameters for Hexagonal and Cubic Mesophases Present in the in Situ Phase Transformation at 150 °C

	2θ (deg)	d (Å)	(hkl)
hexagonal phase: $a = 47.0$ Å	1.97	44.79	(10)
	3.45	25.58	(11)
	3.96	22.29	(20)
	5.23	16.88	(21)
cubic phase: $a = 95.2$ Å	2.05	43.04	(211)
	2.38	37.08	(220)
	3.16	27.93	(321)
	3.39	26.03	(400)
	3.80	23.22	(420)
	3.98	22.17	(332)
	4.14	21.32	(422)
	4.33	20.38	(510)
	4.65	18.98	(521), (440)
	5.23	16.88	(611)
	5.47	16.14	(541)
	5.74	15.38	(631)
	5.98	14.76	(543)

equivalent to the body diagonal of the cubic phase.[12] Orienting MCM-41 and MCM-48 in a similar manner, one observes that the distances between consecutive cylinder axes of MCM-41 are similar to the distances between the body diagonal of MCM-48 and the surrounding helical pore shapes (Figure 2 and Table 1). As has been done previously, the silicate is imagined to be located at the minimal energy surface of MCM-48.[4] The similarities between the H_α/Q_α and MCM-41/-48 transformations indicate that even after polymerizing at room temperature for 3 h, the silicate is still flexible enough to allow surfactant-driven phase transformations to occur. Charge density matching considerations dictate the point at which a clean phase transformation to MCM-48, that is, one in which no other phases are present at the end of the process, will be successful for a given set of concentrations and temperatures.[16] The ideas of charge density matching and extent of silicate polymerization are therefore intertwined.[8]

The difference between the H_α/Q_α and MCM-41/-48 transformations lies in the brief appearance of a lamellar phase during the transformation (Figure 3). Previous

Table 2. Correlation of Unit Cell Parameter g with Observed Liquid-Crystalline Phase[a]

g	aggregate shape
$^1/_3$	sphere
$^1/_2$	cylinder (hexagonal cell, $p6m$ or $p6mm$)
$^1/_2$ to $^2/_3$	bicontinuous surface (cubic cell, $Ia3d$)
1	layer

[a] Based on ref 17.

bulk experiments have indicated that the phase transformation is driven by an increase in the value of the surfactant packing parameter $g = (V)/(a_o)(l)$, where V is the total volume of the surfactant chain plus any cosolvent molecules between the chains, a_o is the effective headgroup area at the organic−inorganic interface, and l is the surfactant chain length.[17] Technically, a fully noninterdigitated surfactant bilayer corresponds to $g = 1$; thus, one would expect a phase transformation to a layered phase to occur from a cubic phase, not a hexagonal one, based on increasing values of g (Table 2). A hexagonal → lamellar transformation runs counter to the phase diagram for the surfactant−water system. Also curious is why such a lamellar phase should disappear once formed; other studies[16] and charge density arguments indicate that layered materials are more polymerized and rigid than hexagonal or cubic phases. In addition, the lamellar phase appeared to be structurally related to the hexagonal and cubic phases since the (100) peak of the lamellar phase occurred in the same location for all experiments (2°−3° 2θ). The lamellar phase most likely arises as a result of the transformation process (see below).[18] Combined with previous data indicating high activation energy barriers for the transformation, these results show that although only a few Si−O−Si bonds need to be broken to accomplish the transformation, the bond breakage process controls the MCM-41/-48 transformation and sets it apart from the surfactant−water system.

(17) (a) Israelachvili, J. N.; Mitchell, D. J.; Ninham, B. W. *J. Chem. Soc., Faraday Trans. 2* **1976**, *72*, 1525. (b) Israelachvili, J. N.; Mitchell, D. J.; Ninham, B. W. *Biochim. Biophys. Acta* **1977**, *470*, 185.

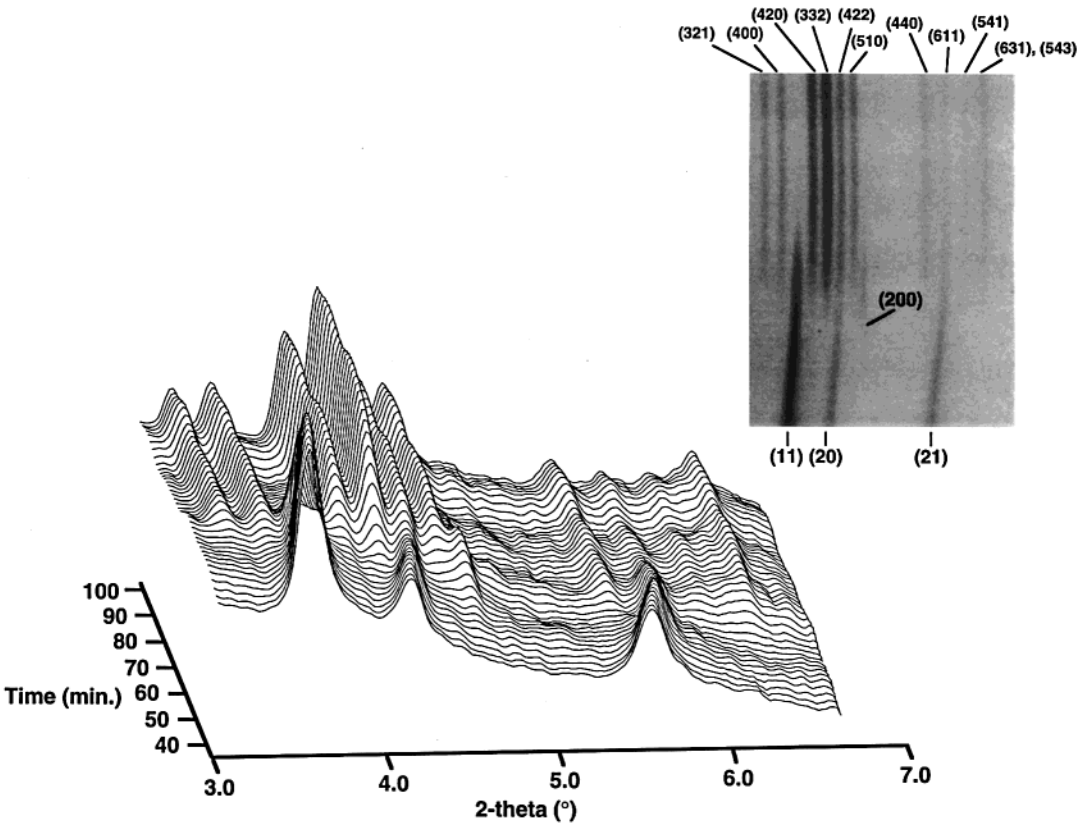

Figure 3. Stacked X-ray diffraction patterns of the MCM-41/-48 phase transformation at 150 °C from 3° to 7° (2θ). The inset shows the indexing of the peaks in this area: bottom, hexagonal $p6m$; top, cubic $Ia3d$. The indexed peak in the center of the inset is from a layered phase that arises and disappears in the phase transformation region.

Model for the Phase Transformation. The short time span (~8 min) over which the $H_\alpha \rightarrow Q_\alpha$ transformation happens provides confirmation of the interconnected pore structure. If one assumes that due to the highly interconnected nature of the system changes in one region are rapidly communicated to neighboring ones, possible results of the transformation process can then be divided into two broad categories depending on whether a topological change is required.

Under the conditions used here, any continuous deformation of the hexagonal MCM-41 structure would necessarily lead to a decrease in g. This is in contrast to the general transformation trends. Any transformations therefore occur as a result of a continuous distortion of the hexagonal phase and must arise as a result of topological changes involving silica restructuring, which enable the silicate wall to sit on a new minimal energy surface,[4] allowing the packing parameter to increase to a higher value. The simplest way to increase g in this manner is by connecting two adjacent cylinders of the hexagonal phase along the cylinder axis (Figure 4). This "cylinder merging" mechanism can naturally propagate to form sheets of increasing width until the assembly meets another one with a different orientation. The persistence of the hexagonal pattern during the transformation period indicates that the occurrence of this hypothetical lamellar structure must be localized in specific areas of the mesophase grains. The lamellar phase was not present in every experiment performed, indicating that it is not necessary for the transformation to occur but appears incidentally during the MCM-41/-48 transformation.

A more elaborate cylinder branching mechanism was initially proposed by Clerc et al. to explain the epitaxial H_α/Q_α phase transformation in $C_{12}EO_6$/water systems.[12] This mechanism is based on structure fluctuations involving the formation of so-called "monkey saddle" towers. The monkey saddle tower is a minimal surface that is periodic in one dimension; its construction has been described by Karcher[19] (Figure 4). The formation of a monkey saddle tower from the hexagonal cylindrical structure can be viewed as a concerted structure rearrangement involving seven neighboring cylinders. These can be divided into two groups of three cylinders arranged symmetrically at (0°, 120°, 240°) and (60°,

(18) There are interesting similarities between the MCM-41 → MCM-48 transformation shown here and $H_\alpha \rightarrow Q_\alpha$ transformations in polyisoprene−polystyrene (PI−PS) diblock copolymers. In some cases, a phase consisting of "hexagonally perforated layers" (HPL) appears during PI−PS $H_\alpha \rightarrow Q_\alpha$ transformations. This phase may be modeled by several mathematical approaches and by combining TEM, SAXS, and SANS with mechanical measurements. Although it is tempting to speculate on the existence of an HPL phase in the MCM−41 → MCM-48 system, there are fundamental differences between the two systems since the surfactant−silica system is not at equilibrium during the phase transformation. The data shown here are much more indicative of the appearance of a simple lamellar phase during the transformation. An HPL phase may be possible, but confirmation of its existence requires more data. See: Qi, S.; Wang, Z.-G. *Phys. Rev. E* **1997**, *55*, 1682. Matsen, M. W.; Bates, F. S. *Macromolecules* **1996**, *29*, 1091. Qi, S.; Wang, Z.-G. *Macromolecules* **1997**, *30*, 4491. Förster, S.; Khandpur, A. K.; Zhao, J.; Bates, F. S.; Hamley, I. W.; Ryan, A. J.; Bras, W. *Macromolecules* **1994**, *27*, 6922. Khandpur, A. K.; Förster, S.; Bates, F. S.; Hamley, I. W.; Ryan, A. J.; Bras, W.; Almdal, K.; Mortensen, K. *Macromolecules* **1995**, *28*, 8796. Gido, S. P.; Wang, Z.-G. *Macromolecules* **1997**, *30*, 6771. Hajduk, D. A.; Harper, P. E.; Gruner, S. M.; Honeker, C. C.; Kim, G.; Thomas, E. L.; Fetters, J. *Macromolecules* **1994**, *27*, 4063. Matsen, M. W.; Schick, M. *Phys. Rev. Lett.* **1994**, *72*, 2660.

(19) Karcher, H. *Manuscr. Math* **1988**, *62*, 83.

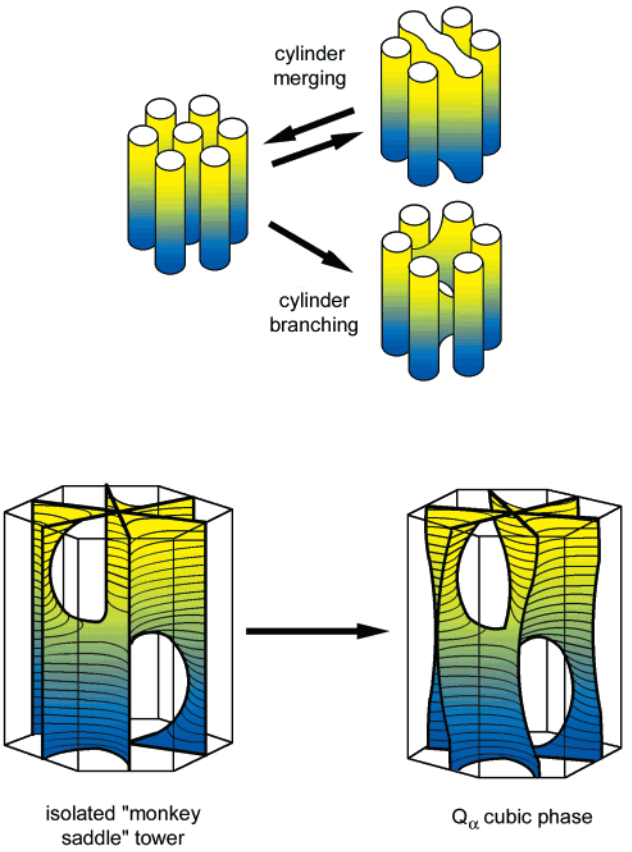

Figure 4. Model for the structural changes occurring during the MCM-41/-48 phase transformation: (a) cylinder merging (top) and cylinder branching (bottom) mechanisms; (b) an illustration of the relationship between the local symmetry of the monkey saddle structure and the *Ia*3*d* cubic phase.

180°, 300°) around a central cylinder. The central cylinder becomes completely disrupted and serves to connect the two groups of cylinders 3 × 3 in an alternating manner. The resulting structure is composed of two interleaved and nonconnecting channels. The silicate surface is locally very similar to the gyroid (G) infinite periodic minimal surface (IPMS)[4,20] found in the cubic phase. A close examination of the 3 × 3 connections reveals that the structure of a given connection is intimately connected to the next nearest connections and must therefore propagate very easily along the cylinder axis, forming a columnar structure. Clerc et al. have also shown that a simple collective distortion of the monkey saddle structure leads to the cubic *Ia*3*d* symmetry or the Q_α and MCM-48 phases.

The data from the present experiment as well as data reported elsewhere[16] yield a model including both cylinder merging and cylinder branching mechanisms, but with different activation energy barriers for each type of transformation. It is likely that both mechanisms operate during the hydrothermal heating of a polymerizing hexagonal mesostructure. The data shown here, in combination with other studies,[16] lead to the conclusion that the cylinder merging mechanism is reversible and kinetically favorable, while the cylinder branching mechanism is thermodynamically more favorable but less reversible. Assuming that the mechanism is sensitive to reaction concentrations and temperature, it is likely for both MCM-48 and a lamellar phase to be observed during transformation of MCM-41. As long as the silicate wall is sufficiently flexible, it is possible for the lamellar phase to revert to the hexagonal phase and from there transform to the cubic phase. However, if the rate of silicate polymerization is sufficiently rapid, the lamellar phase will become "trapped", resulting in a mixture of cubic and lamellar phases. Another way to explain the trapping of the lamellar phase is to invoke an increasing activation energy barrier to the formation of the cubic phase as the silicate become increasingly polymerized. If the hexagonal phase is particularly rigid to begin with, requiring a significant amount of bond breakage for transformation, some hexagonal phase may remain as well. This model thus accounts for reasons why the lamellar phase occasionally persists into the cubic phase, why the lamellar phase tends to occur with a particular *d*-spacing, and why a MCM-41 → lamellar transformation apparently occurs even though it does not appear on the phase diagram of the surfactant−water system.

In Situ Phase Transformations at Temperatures Other Than 150 °C. In situ data from experiments performed at 130 and 170 °C confirm that clean MCM-41/-48 transformations occur at these temperatures (Figure 5). Bulk-phase transformations in the laboratory confirm the in situ results. The data from samples that were successfully produced by the phase transformation process are summarized in Table 3. In general, longer stirring times and shorter heating times are required for the successful synthesis of MCM-48 at higher temperatures. This is due to the increasing activation energy barrier for transformation to the cubic phase as the polymerization of the silica increases; otherwise, the more kinetically favorable lamellar phase, or a mixture of phases, will result as opposed to the thermodynamically favored cubic phase. The stirring time can be viewed as controlling the rigidity of the silicate framework, while the heating time controls the partitioning of alcohol and therefore the rearrangement of the organic region.

We have found that MCM-48 may be produced with less contamination by other phases at higher temperatures rather than lower ones, as judged by the peak intensities and widths in XRD. However, there are benefits to producing the material at 100 °C. For example, a 125-mL Teflon bottle was used for synthesis rather than a 23-mL Parr autoclave, allowing much more material to be produced. In addition, in an industrial setting steam could be used as the heat source, bringing down the cost of production.

Although at each temperature phase-pure MCM-48 is produced, there are some differences among the materials. For example, MCM-48 produced at 190 °C has approximately the same pore diameter as material produced at 100 °C, but the lattice parameter in the latter material is significantly smaller (72.01 Å vs 81.81 Å). This indicates that the amount of silicate separating the pores (wall thickness) is smaller in the 100 °C material. The decrease in wall thickness relative to pore diameter is also reflected in the higher surface area and pore volume of the 100 °C material.

(20) (a) A periodic minimal surface is the smallest surface separating a volume into two equal parts, given a certain periodic constraint. (b) Shoen, A. H. *NASA Technol. Rep. No. 05541*, 1970.

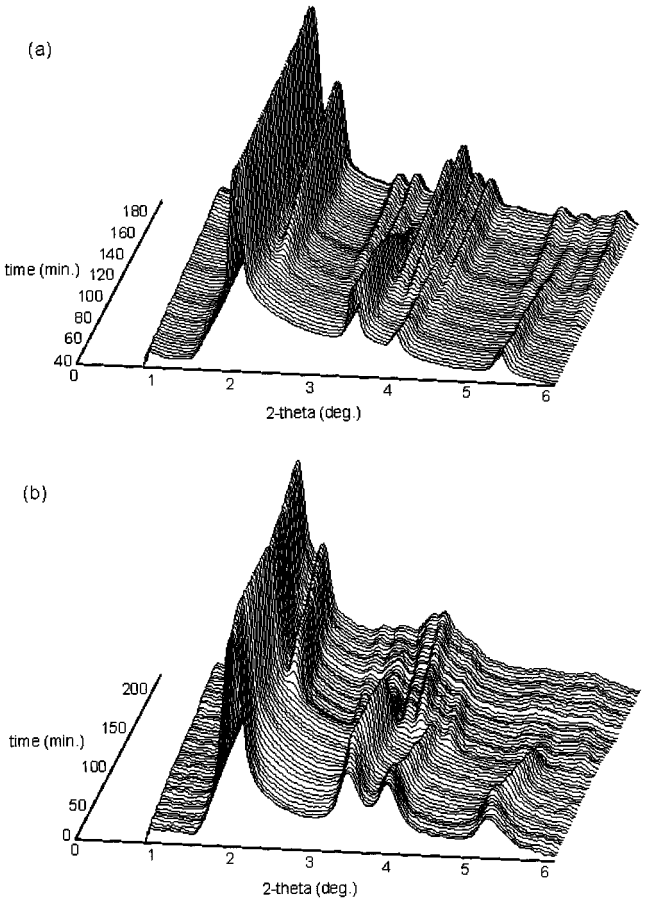

Figure 5. Stacked X-ray diffraction patterns of MCM-41/-48 phase transformations occurring at (a) 130 °C and (b) 170 °C. Stirring times prior to heating are as noted for bulk samples, in Table 3. Note that the phase transformations are continuous in each case and that no lamellar phase arises during the transformation. Diffraction below 1° 2θ is eliminated by the beam stop.

Table 3. Porosity Data and Lattice Parameters for MCM-48 Produced by the Phase Transformation Process at Temperatures between 100 and 190 °C

temp (°C)	stir/heat time[a] (h)	BET surface area (m^2/g)	pore volume (cm^3/g)	BJH pore size (Å)	d(211) (Å)	lattice parameter[b] (Å)
190	4/2	900.99	0.616	25.6	33.4	81.81
170	4/2	901.99	0.545	24.8	31.6	77.40
150	2/4	1028.40	0.594	25.3	30.9	75.69
130	1/5	1233.48	0.651	25.2	29.8	72.99
100	20 min/ 6 days	1237.03	0.817	24.3	29.4	72.01

[a] Based on optimum transformation to MCM-48. [b] Calculated using only d(211).

Bulk-Phase Transformations with Silicate Sources Other Than TEOS. Given that ethanol has been shown to drive the phase transformation of MCM-41 to MCM-48 by increasing the value of g, the presence of other alcohols should also influence the type of phase produced upon heating weakly ordered MCM-41. Bulk experiments were performed in which the alkoxide source was either tetramethyl orthosilicate (TMOS) or tetrapropyl orthosilicate (TPOS). After the mixtures were stirred at room temperature, the TMOS mixture produced MCM-41 while the TPOS mixture produced a lamellar phase. Under conditions where a reaction mixture containing TEOS produced MCM-48 (stir for 2 h and heat for 4 h at 150 °C), the TMOS mixture also produced MCM-48 and the TPOS mixture remained lamellar (Figure 6). These results may be explained by the abilities of the two alcohols produced by these silicate sources to partition into the organic phase and cause an increase in the micellar volume.[21] Methanol is primarily located in the aqueous phase at room temperature and does not interfere with the formation of MCM-41. Upon heating, it penetrates the organic phase much like ethanol, causing phase transformation to MCM-48. The broader peaks of the TMOS−MCM-48 as opposed to TEOS−MCM-48 indicate that the regions of mesoporous ordering are smaller; therefore, methanol is not as effective as ethanol at increasing the packing parameter, as one would expect. Propanol, on the other hand, partitions much more strongly into the organic phase and creates a lamellar phase even at room temperature ($g = 1$). Although a variety of temperatures could be used to transform MCM-41 into MCM-48 when TEOS was used as the alkoxide source, TPOS consistently yielded a layered phase while TMOS produced either a mixture of MCM-41 and -48 or poorly ordered MCM-48.

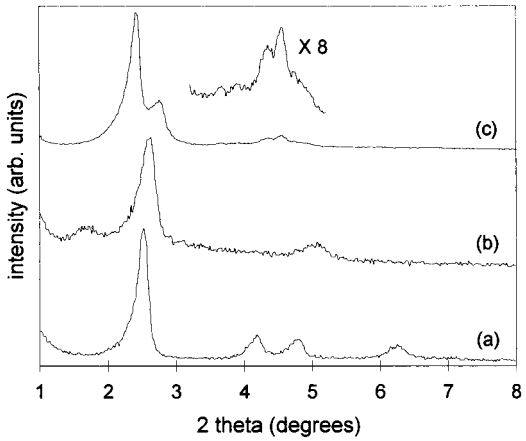

Figure 6. Powder X-ray diffraction patterns of samples from surfactant/silicate mixtures: (a) TMOS as the silicate source, stirred 2 h at room temperature; (b) TPOS as the silicate source, stirred 2 h at room temperature; (c) TMOS as the silicate source, stirred 2 h at room temperature and then heated at 150 °C for 4 h.

Effect of Dissolved Species on the Phase Transformation. Previous research has established the existence of "surfactant-rich" (mesophase) and "surfactant-poor" (aqueous) regions of the reaction system.[22] Since the phase transformation necessarily occurs in a system that is not at equilibrium, it is reasonable to assume that some exchange between the two regions is occurring. Such exchange could be in the form of dynamic surfactant concentrations, where individual surfactant molecules move between the two regions, and could also be shown in the exchange of silicate species.

To examine whether the transformation was entirely independent of the species present in solution, an experiment was performed in which the reaction mixture was stirred for 2 h, the resulting precipitate collected by filtration without completely drying it, and

(21) Riebesehl, W.; Tomlinson, E. *J. Solut. Chem.* **1986**, *15*, 141.
(22) Firouzi, A.; Atef, F.; Oertli, A. G.; Stucky, G. D.; Chmelka, B. F. *J. Am. Chem. Soc.* **1997**, *119*, 3596.

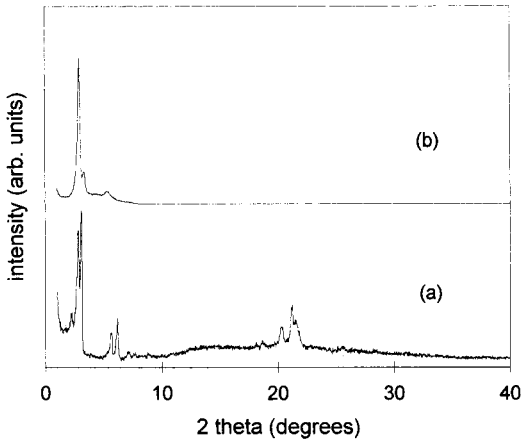

Figure 7. Powder X-ray diffraction patterns of samples from surfactant/silicate mixtures using TEOS as the silicate source: (a) stirred 2 h at room temperature, filtered, resuspended in 15 mL of aqueous solution at pH 11, and heated for 4 h at 150 °C; (b) stirred 2 h at room temperature, filtered, resuspended in the supernatant from an identically prepared mixture, heated for 4 h at 150 °C, then filtered, and calcined in air.

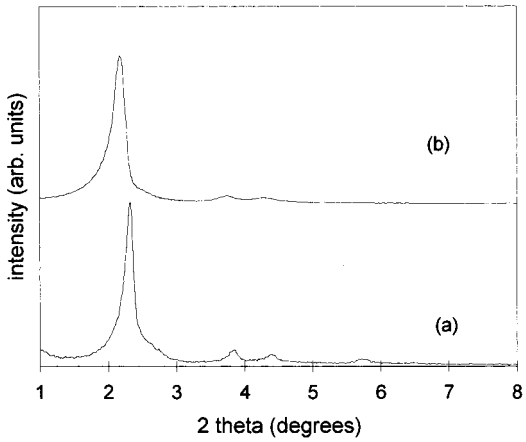

Figure 8. Powder X-ray diffraction patterns of samples using TEOS as the silicate source, stirred 2 h/heated 4 h at 150 °C: (a) NaF added; (b) $Al(O^iPr)_3$ added.

then resuspended in an identical amount of a solution at the same pH as the reaction mixture (i.e., only OH^- was present; CTAB, silicate, and ethanol were not). The mixture was then transferred to a Parr autoclave and heated at 150 °C for 4 h. The result is shown in Figure 7. This diffraction pattern is most similar to layered silicate minerals such as ilerite, magadiite, and kanemite that have been intercalated with CTAB.[23] In contrast, fully polymerized MCM-41 subjected to identical reaction conditions did not show a significant change in structure. This result shows that the solution chemistry also plays an important role in the phase transformation. This role is complementary to the charge density matching and degree of silicate polymerization, which play a more intimate role within the composite.

Additional confirmation of the participation of the dissolved species in the phase transformation is provided by an experiment in which two identical reaction mixtures were stirred for 2 h, the damp precipitates were collected on separate filters, and the supernatants were saved. The solids were each resuspended in the *other* supernatant, transferred to Parr autoclaves, and heated at 150 °C for 4 h. In this case, each reaction mixture produced a mixture of a layered phase and MCM-48; calcination caused collapse of the layered phase, leaving only MCM-48 (Figure 7). Regardless of origin, as long as the concentration and identity of solution species is correct, the transformation will proceed according to the model described above. Tests to identify the types and concentrations of species present in the solution phase are currently in progress.

Effect of Inorganic Framework Rigidity. Several recent articles have shown that the addition of small amounts of fluoride to the synthesis of silicate mesostructures can produce interesting structural changes.[24] Fluoride acts as a mineralizer, producing silicate with a higher degree of polymerization than materials produced without it. To further explore the role of silicate polymerization on the phase transformation process, reaction mixtures were prepared with a 5.12:1.00 mole ratio of SiO_2:F^-, using either NH_4F, NaF, or $NH_4F{\cdot}HF$ as the fluoride source. Mixtures were then stirred and heated for 2 and 4 h (150 °C), respectively. The powder XRD of the product (Figure 8) shows that no phase transformation occurred even in the presence of ethanol. ^{29}Si MAS NMR spectra of the material isolated just prior to heating shows a higher degree of polymerization than material from a mixture without fluoride, as evidenced by the higher Q_4/Q_3 ratio. We also found that when successively smaller and smaller amounts of fluoride were added, increasing amounts of MCM-48 appeared along with the MCM-41 (as measured by the relative intensity of the $d(100)$ peak of the H_α phase and the $d(211)$ peak of the Q_α phase) until when $[F^-] = 0$, pure MCM-48 was produced. These results confirm the important role of silicate polymerization in the transformation process; alcohol partitioning is not the only determining factor.

The same result was obtained when an aluminum source was added to the reaction mixture. Recent research has shown that Al−MCM-41 may be prepared with unusually high concentrations of tetrahedral aluminum (Si:Al = 8:1, 4:1, 2:1, 1:1) by using aluminum isopropoxide, $Al(O^iPr)_3$, as the Al source and aging for 1 h in base prior to the addition of the silicate source.[25] To test the phase transformation ability of these materials, a reaction mixture was prepared that was identical to those described elsewhere in the paper where TEOS was used, except that $Al(O^iPr)_3$ was added to the reaction mixture at a SiO_2:Al_2O_3 ratio of 16:1. The Al source was aged in basic solution as indicated; the complete reaction mixture was then stirred for 2 h

(23) Landry, C. C.; Stucky, G. D., unpublished results.

(24) (a) Voegtlin, A. C.; Ruch, F.; Guth, J. L.; Patarin, J.; Huve, L. *Microporous Mater.* **1997**, *9*, 95. (b) Guth, J. L.; Kessler, H.; Wey, R. *Stud. Surf. Sci. Catal.* **1986**, *28*, 121. (c) Jeong, S. Y.; Suh, J. K.; Lee, J. M.; Kwon, O. Y. *J. Colloid Interface Sci.* **1997**, *192*, 156. (d) Silva, F. H. P.; Pastore, H. O. *J. Chem. Soc., Chem. Commun.* **1996**, 833. (e) Prouzet, E.; Pinnavaia, T. J. *Angew. Chem., Int. Ed. Engl.* **1997**, *36*, 516.

(25) (a) Carrazza, J.; González, F.; Adrián, R.; Djaouadi, D.; Moore, J. G.; Shahriari, D. Y.; Landry, C. C.; Lujano, J. *Proceedings 12th International Zeolite Conference*; Treacy, M. M. J., Marcus, B. K., Bisher, M. E., Higgins, J. B., Eds.; MRS Publishing: Warrendale, PA, 1999; Vol. 2, p 801. (b) Janicke, M. T.; Landry, C. C.; Christiansen, S. C.; Kumar, D.; Stucky, G. D.; Chmelka, B. F. *J. Am. Chem. Soc.* **1998**, *120*, 6940. (c) Janicke, M. T.; Landry, C. C.; Christiansen, S. C.; Birtalan, S.; Stucky, G. D.; Chmelka, B. F. *Chem. Mater.* **1999**, *11*, 1342.

and heated at 150 °C for 4 h. The XRD of the resulting material is strikingly similar to that obtained from the sample prepared in the presence of fluoride; the phase remains MCM-41, and the high peak intensities and narrow peak widths indicate large regions of ordering (Figure 8). The incorporation of Al into the inorganic framework, even though it necessarily adds negative charge, does not encourage the phase transformation on a charge density matching basis. It is also important to note that since an aluminum alkoxide was used as the Al source, almost twice as much total alcohol (2-propanol or ethanol) was present per tetrahedral framework atom (Si or Al) than in a normal transformation synthesis. These factors indicate that it is probably not possible to use the phase transformation method to successfully make Al−MCM-48 with catalytically useful concentrations of aluminum (Si:Al > 8:1) in this amorphous aluminosilicate framework.

Conclusions

We have learned that the MCM-41/-48 phase transformation happens in an epitaxial manner, with coherent registry of one phase to the other and without dissolution of the initially formed MCM-41. Two competing mechanisms, one involving longitudinal linkage of hexagonal pores (cylinder merging) and the other involving transverse linkage (cylinder branching), can be proposed for the transformation. The kinetic product is the lamellar phase, while the cubic phase is thermodynamically favored. Adjustment of synthetic parameters to account for the activation energy barriers for each mechanism can allow the bulk synthesis of MCM-48 at a variety of temperatures between 100 and 190 °C by the phase transformation of MCM-41. An overall model where both processes operate simultaneously and in an intimately connected manner can explain the appearance of a lamellar phase during the in situ transformation at 150 °C.

Importantly, these results provide support for the view of a highly cooperative self-assembly process. Previous results confirmed the role of the organic component, through modification of *g*. Data in this paper confirm this role, but also show that the inorganic component, while not directly controlling the type of mesostructure produced, does play an important part in determining whether a phase transformation will occur at all. This appears to be accomplished mainly through the extent of silicate polymerization and to some extent charge density matching.

Acknowledgment. This work was funded by the NSF under Grants CHE-9875768, DMR-9634396, and DMR-9520971, by the NSF EPSCoR program under Cooperative Agreement EPS-9874685, and by the University of Vermont through start-up funding. Research at Brookhaven was supported under Contract DE-AC02-98CH10886 with the U.S. Department of Energy by its division of Chemical Sciences, Office of Basic Energy Research. The authors with to express their strong appreciation to Dr. Bradley Chmelka for his insight and useful discussions.

CM000373Z